



OPEN

# Taurine, alpha lipoic acid and vitamin B6 ameliorate the reduced developmental competence of immature mouse oocytes exposed to methylglyoxal

Saba Mokhtari<sup>1</sup>, Amir Hossein Mahdavi<sup>1</sup>✉, Farnoosh Jafarpour<sup>2</sup>, Mohsen Rahimi Andani<sup>2</sup>, Maurizio Dattilo<sup>3</sup> & Mohammad Hossein Nasr-Esfahani<sup>2</sup>✉

Advanced glycation end products (AGEs) are the final products of the Maillard reaction, formed through the interaction of carbohydrates and proteins. Reactive dicarbonyl compounds such as methylglyoxal (MGO) serve as precursors for AGEs formation. Elevated levels of MGO/AGEs are observed in conditions like obesity, polycystic ovarian syndrome (PCOS), and diabetes, negatively impacting oocyte development. Previous studies have shown that hydrogen sulfide, a gasotransmitter with anti-AGEs effects, is produced in a process influenced by vitamin B6. R- $\alpha$ -lipoic acid (ALA) inhibits protein glycation and AGEs formation while stimulating glutathione (GSH) production. Taurine mitigates oxidative stress and acts as an anti-glycation compound, preventing in vitro glycation and AGEs accumulation. This study aimed to explore the ameliorative effects of a micronutrient support (Taurine, ALA and B6: TAB) on mouse oocytes challenged with MGO. Our results indicate that MGO reduces oocyte developmental competence, while TAB supplementation improves maturation, fertilization, and blastocyst formation rates. TAB also restores cell lineage allocation, redox balance and mitigates mitochondrial dysfunction in MGO-challenged oocytes. Furthermore, cumulus cells express key enzymes in the transsulfuration pathway, and TAB enhances their mRNA expression. However, TAB does not rescue MGO-induced damage in denuded oocytes, emphasizing the supportive role of cumulus cells. Overall, these findings suggest that TAB interventions may have significant implications for addressing reproductive dysfunctions associated with elevated MGO/AGEs levels. This study highlights the potential of TAB supplementation in preserving the developmental competence of COCs exposed to MGO stress, providing insights into mitigating the impact of dicarbonyl stress on oocyte quality and reproductive outcomes.

**Keywords** Advanced glycation end products, Alpha lipoic acid, Cumulus oocyte complex, Denuded oocyte, Maturation, Methylglyoxal, Taurine, Vitamin B6

Advanced glycation end products (AGEs) are the final products of the Maillard reaction, a chemical process between carbohydrates and proteins. like methylglyoxal (MGO), glyoxal (GO), and 3-deoxy-glucose (3-DG) are reactive dicarbonyl compounds that serve as precursors for AGEs formation<sup>1,2</sup>. AGEs are produced endogenously under conditions, such as hyperglycemia, insulin resistance, obesity, oxidative stress, hypoxia, and aging<sup>1</sup>, which enhance their formation within the body. Additionally, exogenous sources particularly thermal food processing, contribute significantly to AGE production<sup>3</sup>. Consumption of foods rich in AGEs poses potential risks to public health<sup>1-3</sup>.

MGO is recognized as a significant and reactive precursor in the formation of AGEs<sup>4,5</sup>. Elevated levels of MGO and AGEs have been observed in individuals with conditions such as obesity, polycystic ovarian syndrome

<sup>1</sup>Department of Animal Science, College of Agriculture, Isfahan University of Technology, Isfahan, Iran. <sup>2</sup>Department of Animal Biotechnology, Reproductive Biomedicine Research Center, Royan Institute for Biotechnology, ACECR, Isfahan, Iran. <sup>3</sup>Parthenogen, Lugano, Switzerland. ✉email: mahdavi@iut.ac.ir; mh.nasr-esfahani@royaninstitute.org

(PCOS), and diabetes compared to healthy individuals<sup>1,6,7</sup>. This suggests that these conditions are associated with either increased production or impaired clearance of MGO, leading to heightened AGEs formation. Obesity is often accompanied by insulin resistance and metabolic dysfunction, contributing to elevated MGO and AGEs levels. Similarly, PCOS is linked to insulin resistance and metabolic disturbances, which may exacerbate MGO and AGEs accumulation<sup>7,8</sup>. Measurement of MGO and AGEs levels in serum or follicular fluid provides insights into the metabolic and pathophysiological changes associated with these conditions<sup>1,6</sup>. Elevated levels of MGO and AGEs in these fluids indicate increased glycation and oxidative stress, which can adversely affect cellular function and contribute to the development of complications linked to these metabolic disorders<sup>1,6–8</sup>.

The receptor for AGEs (RAGE) plays a pivotal role in mediating the cellular effects of MGO and AGEs. Studies suggest that the AGE-RAGE system may contribute to abnormal female reproductive functions, particularly in conditions such as PCOS and diabetes<sup>1</sup>. In these conditions, the interaction between could potentially impair follicular growth, reduce the number and quality of retrieved oocytes, and diminish the developmental competence of oocytes, ultimately affecting pregnancy rate.

Research has demonstrated that exposure of oocytes to MGO can lead to reduced developmental competence<sup>9–11</sup>. This outcome may be attributed to several factors, including disturbances in mitochondrial distribution<sup>9,11</sup>, alterations in cellular redox state<sup>9,10</sup>, elevated levels of lipid peroxidation<sup>10</sup>, and depletion of glutathione (GSH) content<sup>11</sup>.

Hydrogen sulfide ( $H_2S$ ) is recognized as the third gasotransmitter, alongside nitric oxide (NO) and carbon monoxide (CO).  $H_2S$  is enzymatically produced from homocysteine, primarily by three enzymes: cystathione  $\beta$ -synthase (CBS), cystathione  $\gamma$ -lyase (CSE), and 3-mercaptopropane sulfurtransferase (3-MPST). CBS and CSE are predominantly located in the cytoplasm, while 3-MPST is situated in the mitochondria<sup>4,12–15</sup>. These enzymes play crucial roles in the transsulfuration pathway, which is integral to one-carbon metabolism. CBS and CSE specifically regulate the partitioning of homocysteine between the re-methylation pathway and the transsulfuration pathway.

Vitamin B6 function as a crucial cofactor for the enzymes CBS and CSE in the transsulfuration pathway, which is responsible for the endogenous production of  $H_2S$ . This vitamin plays a vital role in facilitating the enzymatic conversion of cysteine into  $H_2S$ <sup>16</sup>. Additionally, within the transsulfuration pathway, there is an alternative route where excess cysteine can be converted to taurine by the enzyme cysteine dioxygenase (CDO)<sup>16,17</sup>.

Several studies have highlighted  $H_2S$ 's potential anti-AGEs effects. Specifically, researches indicate that  $H_2S$  can mitigate the toxicity associated with the RAGE by inhibiting its dimer formation and destabilizing its structure. These findings suggest that  $H_2S$  may play a protective role against cellular damage induced by AGEs<sup>18,19</sup>.

R- $\alpha$ -lipoic acid (ALA) serves as the biologically active form and essential cofactor in mitochondrial respiratory enzymes. ALA has been extensively studied for its ability to inhibit protein glycation, formation of AGEs, and modulation of RAGE expression. By preventing AGEs formation, ALA may mitigate the detrimental effects associated with AGEs accumulation in tissues<sup>20</sup>. Furthermore, ALA has been shown to stimulate GSH production. This antioxidant property of ALA is crucial as it facilitates the reduction of cystine to cysteine, a precursor of GSH<sup>21,22</sup>. Increased GSH levels contribute to cellular antioxidant defenses.

Given the significant implications of AGEs and MGO in various pathophysiological conditions such as hyperglycemia, insulin resistance, and obesity, there is growing interest in understanding dicarbonyl stress and its impact on reproductive aspects. Dicarbonyl stress has been linked to disturbances in the transsulfuration pathway, potentially reducing endogenous  $H_2S$  production. This disruption in cellular redox balance can impair  $H_2S$ 's role as a signaling molecule.

Based on these findings, our study aims to investigate the potential ameliorating effects of TAB interventions on the developmental competence of mouse oocytes challenged with MGO. By utilizing these interventions, we hope to mitigate the negative impact of MGO on oocyte development. The results of this study could have implications for understanding and potentially addressing reproductive dysfunctions in individuals challenged with conditions such as obesity, PCOS, and diabetes where elevated levels of MGO/AGEs may be present.

## Results

### MGO diminishes the developmental competence of cumulus oocyte complexes (COCs)

To investigate the developmental competence of immature COCs exposed to MGO, we cultured COCs in the presence of various concentrations of MGO, including 0.0, 20, 40, 75, and 150  $\mu$ M. After 18 h (h), maturation rates were assessed in 6 experimental replicates, with approximately 50 oocytes per replicate in each experimental group.

In Fig. 1A, the proportion of oocytes that reached the metaphase meiosis II (MII) stage (maturation rate) after in vitro maturation (IVM) with 20  $\mu$ M ( $50.88 \pm 2.31\%$ ) and 40  $\mu$ M ( $52.89 \pm 1.72\%$ ) MGO was statistically similar to the control group ( $58.42 \pm 4.60\%$ ) ( $P > 0.05$ ). However, a significantly lower maturation rate was observed in the 75  $\mu$ M and 150  $\mu$ M MGO groups, with reductions of  $36.05 \pm 0.73\%$  and  $21.62 \pm 10.65\%$  compared to the control ( $P < 0.05$ ). To assess the developmental competence of matured COCs exposed to different MGO concentrations, in vitro fertilization (IVF) was performed, and the rate of pronucleus formation (zygotes with two defined male and female pronucleus: 2PN) was evaluated 6 h after fertilization (Fig. 1B). The results revealed a significant decrease in the ability of oocytes to be fertilized by fresh sperm in the 75  $\mu$ M and 150  $\mu$ M MGO groups ( $30.68 \pm 3.18\%$  and  $15.25 \pm 9.96\%$ , respectively) compared to the control group ( $53.07 \pm 7.58\%$ ) ( $P < 0.05$ ). Subsequently, the blastocyst formation rate was assessed after 4.5 days of in vitro culture (IVC) following the IVF procedure. Figure 1C shows that the blastocyst formation rates in the 75  $\mu$ M and 150  $\mu$ M MGO groups ( $6.06 \pm 0.95\%$  and  $4.87 \pm 2.88\%$ , respectively) were significantly lower than that of the control, 20  $\mu$ M, and 40  $\mu$ M MGO groups ( $22.19 \pm 5.20\%$ ,  $23.46 \pm 2.16\%$ , and  $17.39 \pm 4.63\%$ , respectively) ( $P < 0.05$ ).

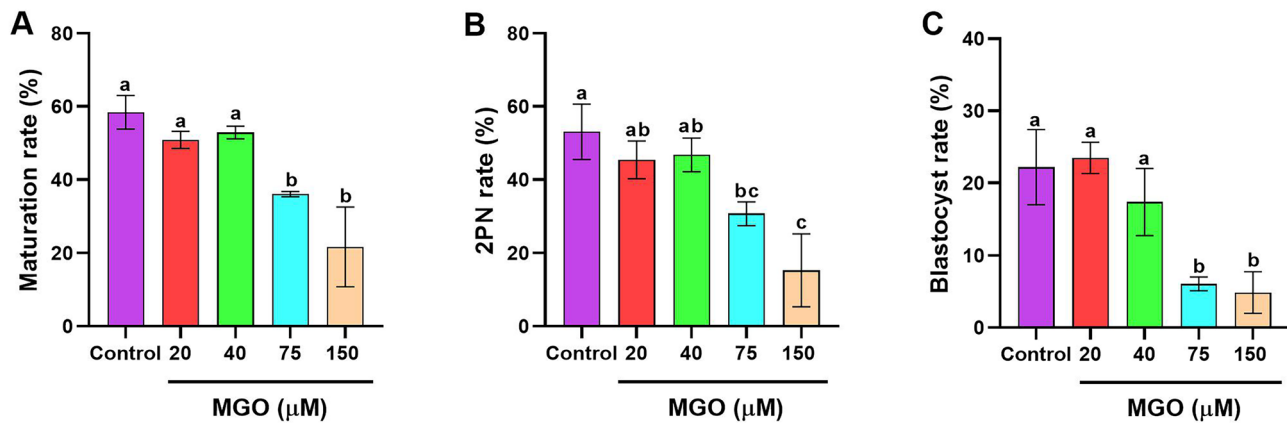


**Figure 1.** MGO diminishes the developmental competence of COCs. COCs were cultured in IVM medium with indicated concentrations of MGO (20, 40, 75 and 150  $\mu\text{M}$ ) for 16–18 h and then IVF was carried out on matured COCs and then cultured in G-TL medium for 4.5 days; (A) Maturation rate/ GV, (B) 2PN formation rate/ GV and (C) Blastocyst rate/ GV; At least 50 COCs were cultured in each replicate of each treatment group. Five replicates were included. Data are presented as means  $\pm$  SEM. Different letters (a, b, and c) indicate significant differences between the treatment groups at  $P < 0.05$ . Statistical differences between groups were assessed using one-way ANOVA with LSD post-hoc test.

#### Taurine, ALA, and B6 (TAB) supplementation improves the developmental competence of matured COCs exposed to MGO stress

To investigate whether the combination of Taurine, ALA, and B6 (TAB) could ameliorate the reduced developmental competence of COCs exposed to MGO stress, immature COCs were co-treated with MGO and TAB. Among the tested concentrations of MGO, both 75  $\mu\text{M}$  and 150  $\mu\text{M}$  significantly reduced the maturation rate and developmental competence of the challenged COCs. Considering that 75  $\mu\text{M}$  MGO represents a concentration closer to in vivo condition, we selected this concentration for co-treatment with TAB in the subsequent part of this study to explore the potential beneficial effects of TAB on COCs exposed to MGO stress during IVM. In addition, the concentration of taurine, ALA, and B6 used in this study as components of the TAB cocktail was 10 mM, 10  $\mu\text{M}$ , and 10  $\mu\text{M}$ , respectively, based on our findings and previous studies<sup>21,23,24</sup>.

As shown in Fig. 2 (A-C), we observed that COCs exposed to MGO stress (75  $\mu\text{M}$ ) co-treated with TAB cocktail improved all assessed developmental aspects including maturation ( $36.68 \pm 7.10\%$  vs.  $55.34 \pm 5.26\%$ ), 2PN formation ( $26.63 \pm 4.57\%$  vs.  $45.21 \pm 0.52\%$ ) and blastocyst ( $4.92 \pm 2.77\%$  vs.  $28.09 \pm 5.27\%$ ) rate compared to 75  $\mu\text{M}$  MGO group.

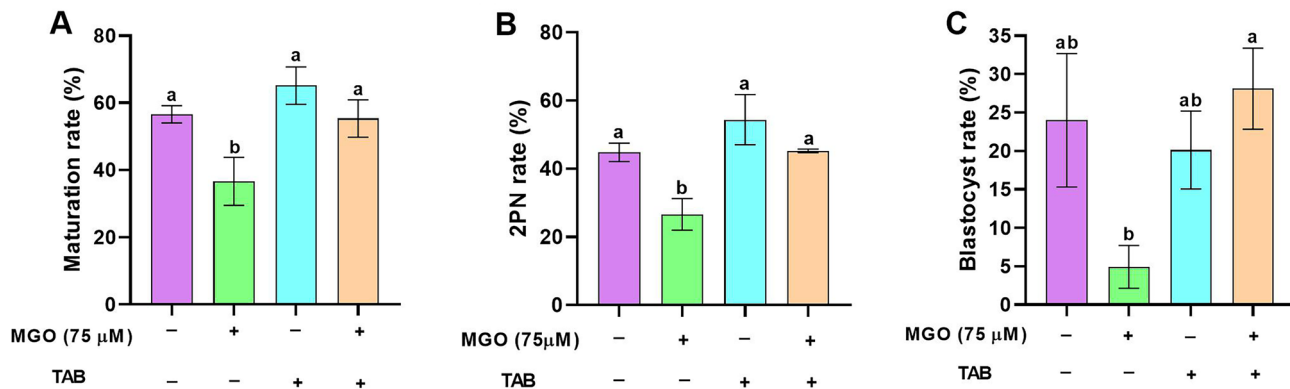


**Figure 2.** Supplementation of IVM medium with TAB cocktail (Taurine, ALA, and B6) improves the developmental competence of matured COCs exposed to MGO stress. COCs were cultured in IVM medium with indicated concentrations of MGO (75  $\mu\text{M}$ ) and/or TAB (Taurine: 10 mM; ALA: 10  $\mu\text{M}$  and B6: 10  $\mu\text{M}$ ) for 16–18 h and then IVF was carried out on matured COCs and then cultured in G-TL medium for 4.5 days; (A) Maturation rate/ GV, (B) 2PN formation rate/ GV and (C) Blastocyst rate/ GV; At least 50 COCs were cultured in each replicate of each treatment group. Five replicates were included. Data are presented as mean  $\pm$  SEM. Different letters (a and b) indicate significant differences between the treatment groups at  $P < 0.05$ . Statistical differences between groups were assessed using one-way ANOVA with LSD post-hoc test.

### TAB cocktail restored impaired cell lineage allocation in blastocysts developed from COCs exposed to MGO stress

In Fig. 3, blastocysts derived from COCs exposed to 75  $\mu$ M MGO stress for 4.5 days exhibited reductions in inner cell mass ( $12.31 \pm 1.31\%$  vs.  $16.66 \pm 2.02\%$ ) (Fig. 3A), trophectoderm ( $21.79 \pm 1.95\%$  vs.  $30.10 \pm 2.36\%$ ) (Fig. 3B) and total cell number ( $34.10 \pm 2.79\%$  vs.  $46.26 \pm 3.69\%$ ) (Fig. 3C) compared with the control group ( $P < 0.05$ ). Co-treatment with the TAB cocktail effectively mitigated these effects, resulting in improved inner cell mass ( $19.26 \pm 0.85\%$  vs.  $12.31 \pm 1.31\%$ ) (Fig. 3A), trophectoderm ( $28.84 \pm 2.76\%$  vs.  $21.79 \pm 1.95\%$ ) (Fig. 3B), and total cell number ( $48.10 \pm 3.54\%$  vs.  $34.10 \pm 2.79\%$ ) (Fig. 3C) compared to 75  $\mu$ M MGO group ( $P < 0.05$ ) and no significant different from the control group ( $P > 0.05$ ).

### TAB cocktail restored the perturbed redox balance in COCs exposed to MGO stress

Previously studies, have established that MGO induces oxidative stress. As shown in Fig. 4, treatment with 75  $\mu$ M MGO significantly increased ROS levels and reduced GSH levels in COCs ( $29.41 \pm 1.67$  vs.  $20.34 \pm 1.67$ , and  $58.51 \pm 2.87$  vs.  $75.12 \pm 3.12$ , respectively) (Fig. 4A,C, respectively;  $P < 0.05$ ). To investigate whether the impaired redox state could be restored in matured COCs using the TAB cocktail, we co-treated the MGO-challenged COCs with TAB during IVM. Interestingly, co-treatment with TAB resulted in a significant reduction in ROS levels and an increase in GSH levels compared to MGO-challenged COCs ( $22.09 \pm 1.14$  vs.  $29.49 \pm 1.67$ , and  $78.17 \pm 2.87$  vs.  $58.51 \pm 2.87$ , respectively) ( $P < 0.05$ , Fig. 4). These values were comparable to those observed in the control group. Additionally, supplementing the IVM medium with TAB in the absence of MGO did not significantly alter ROS levels ( $23.15 \pm 1.23$  vs.  $20.34 \pm 1.37$ ) (Fig. 4A,B,  $P > 0.05$ ) but significantly increased GSH levels compared to the control group ( $109.56 \pm 3.49$  vs.  $75.12 \pm 3.12$ ) ( $P < 0.05$ ).

### TAB cocktail mitigates the mitochondrial dysfunction in MGO-challenged COCs

In this study, we investigated the impact of MGO on mitochondrial function in COCs, focusing on the mitochondrial mass index (MMI) and mitochondrial membrane potential (MMP). We utilized MitoTracker Green dye and the JC-1 kit to assess MMI and MMP, respectively. As depicted in Fig. 5, treatment with 75  $\mu$ M MGO significantly decreased both MMI ( $7.96 \pm 0.20\%$  vs.  $9.47 \pm 0.42\%$ ) (Fig. 5A,B) and the MMP ( $1.15 \pm 0.10\%$  vs.  $1.74 \pm 0.08\%$ ) (Fig. 5C,D) in matured COCs compared to the control group ( $P < 0.05$ ). Interestingly, co-treatment

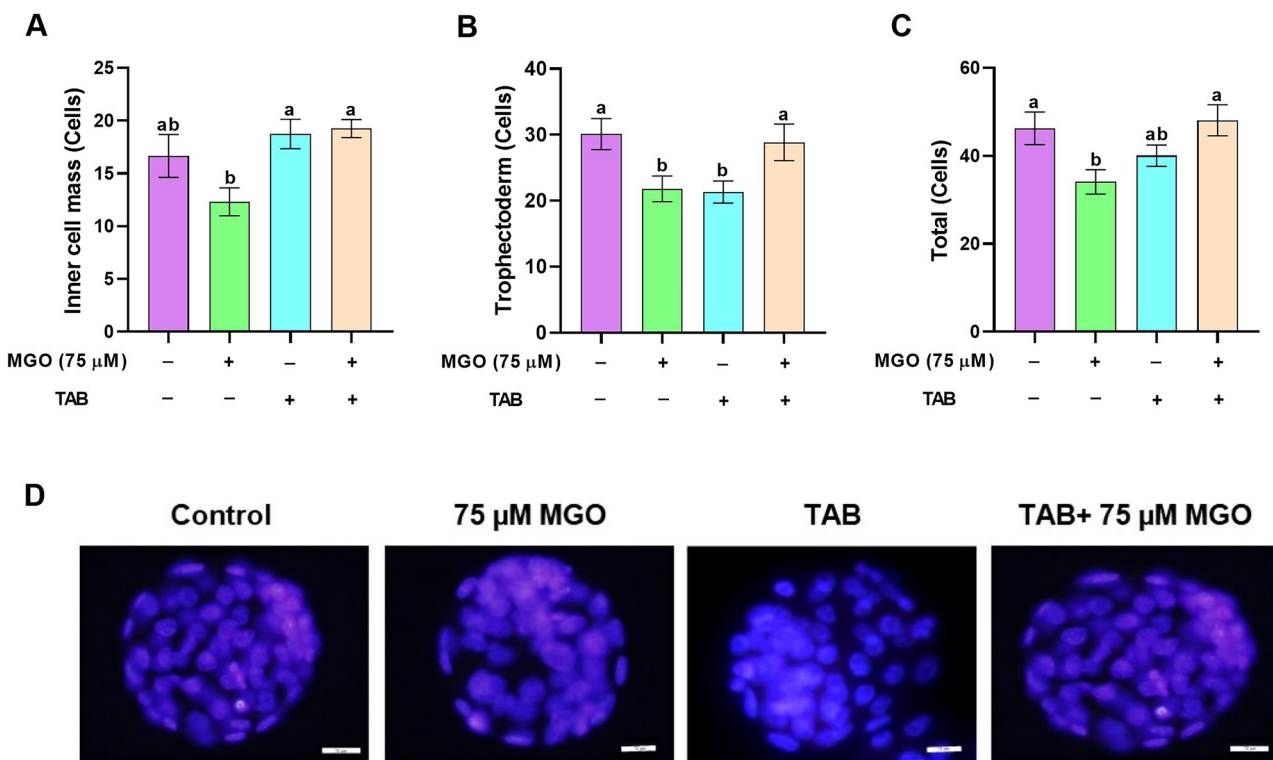


**Figure 3.** TAB cocktail restores impaired cell lineage allocation in blastocysts developed from COCs exposed to MGO stress. COCs were cultured for 16–18 h in IVM medium containing MGO (75  $\mu$ M) and/or TAB, and then fertilized in vitro and then cultured in G-TL medium for 4.5 days, (A) Inner cell mass (ICM), (B) trophectoderm (TE) and (C) Total cell numbers (TCN) were counted in each blastocyst. (D) Representative images show the ICM cells in red and TE cells in pink. The number of stained blastocysts was 30 in each group. The scale bars represent 20  $\mu$ m. Data are presented as means  $\pm$  SEM. Different letters (a and b) indicate significant differences between the treatment groups at  $P < 0.05$ . Statistical differences between groups were assessed using one-way ANOVA with LSD post-hoc test.

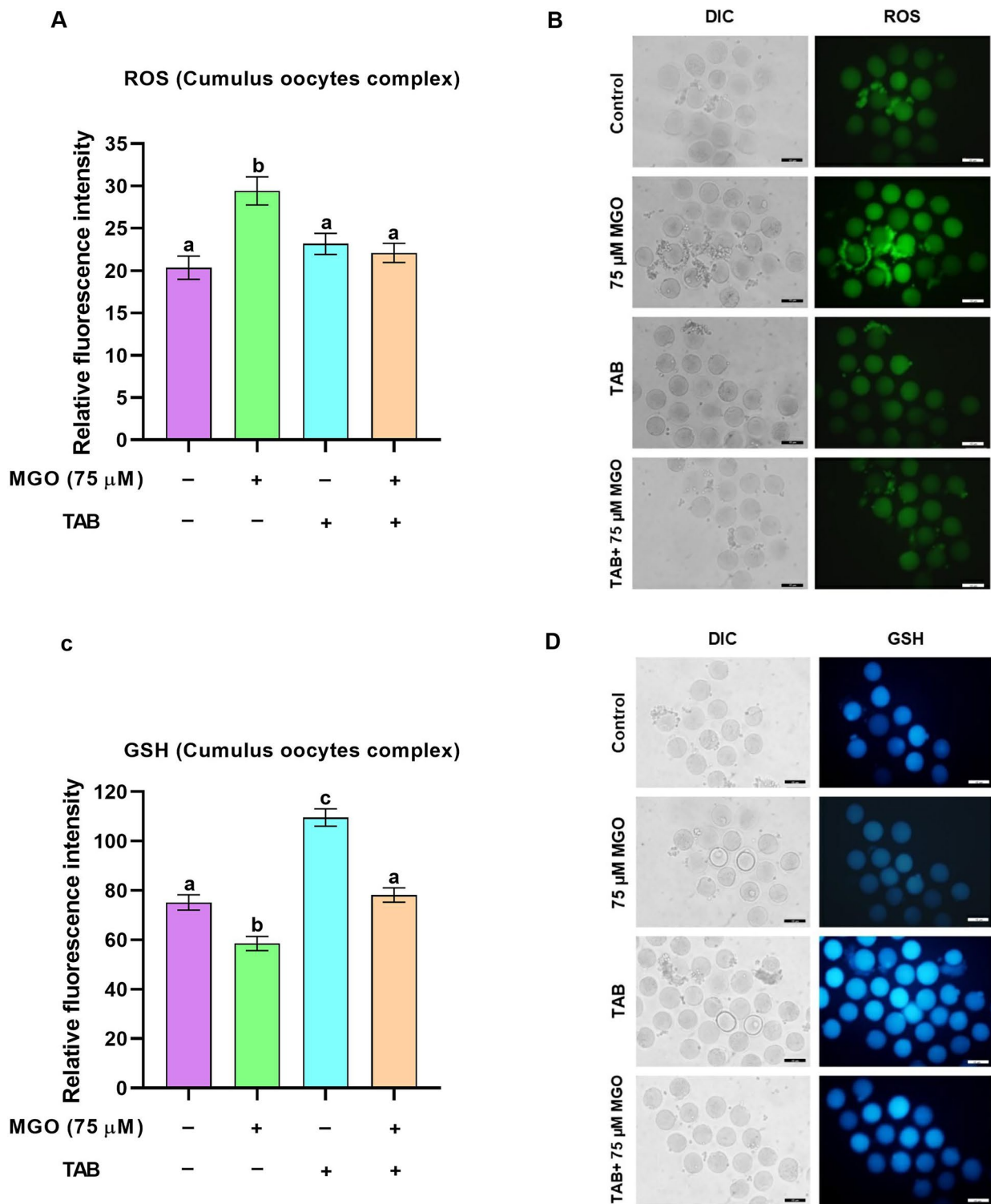


**Figure 4.** TAB cocktail restores the impaired redox balance in COCs exposed to MGO stress. The relative fluorescence intensity of (A) ROS and (C) GSH levels in matured oocytes, (B) The representative images show the ROS levels, and (D) GSH levels using a fluorescence microscope. Number of stained oocytes was 20 in each replicate of each treatment group. Five replicates were included. The scale bars represent 50  $\mu$ m. Data are presented as means  $\pm$  SEM. Different letters (a, b, and c) indicate significant differences between the treatment groups at  $P < 0.05$ . Statistical differences between groups were assessed using one-way ANOVA with LSD post-hoc test.

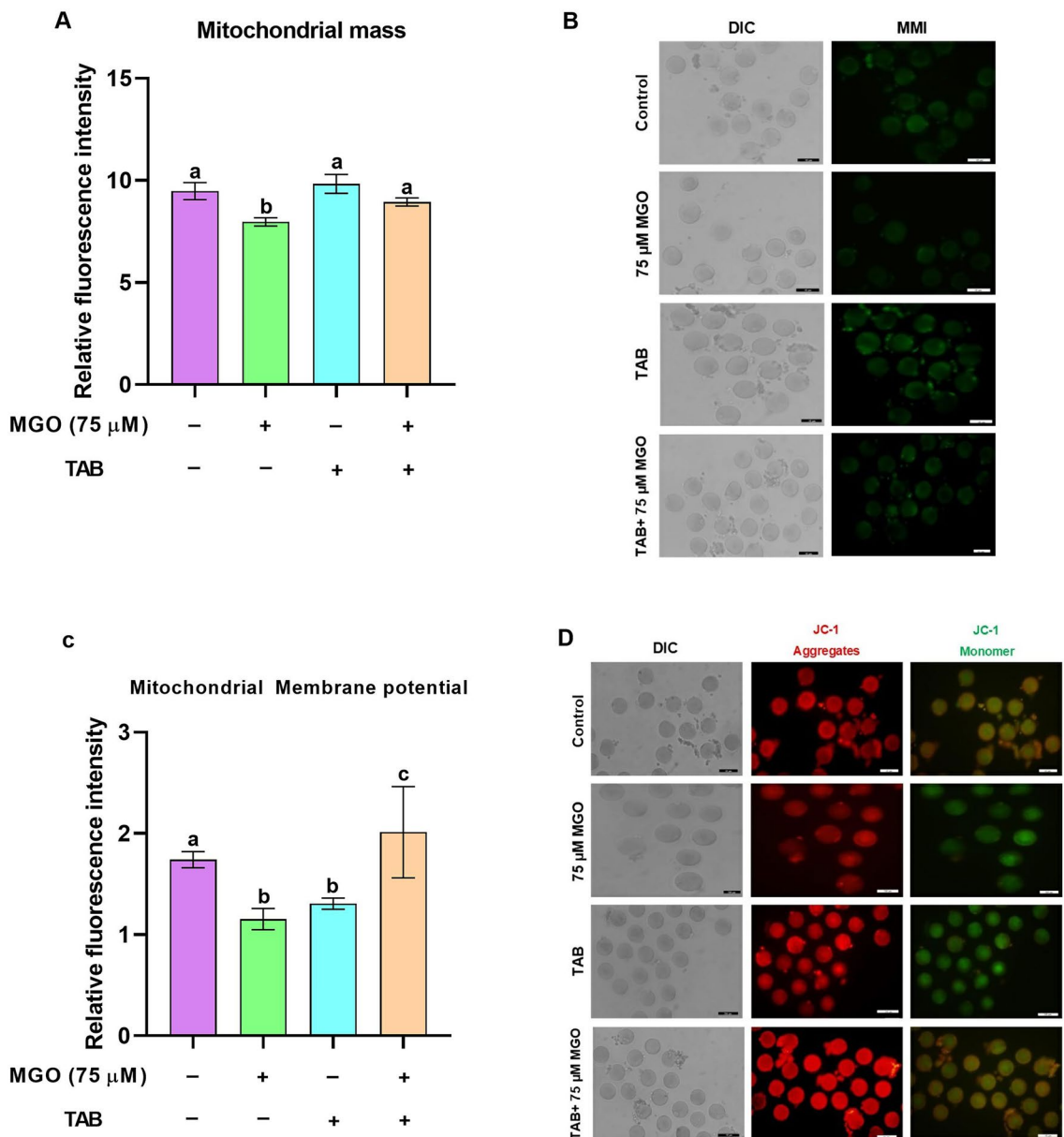


**Figure 5.** TAB cocktail mitigates the mitochondrial dysfunction in MGO-challenged COCs. The relative fluorescence intensity of (A) mitochondrial mass and (C) mitochondrial membrane potential. (B) The representative images showed mitochondrial mass and (D) mitochondrial membrane potential using a fluorescence microscope. Number of stained oocytes was 20 in each replicate of each treatment group. Five replicates were included. The scale bars represent 50  $\mu$ m. Data are presented as means  $\pm$  SEM. Different letters (a, b, and c) indicate significant differences between the treatment groups at  $P < 0.05$ . Statistical differences between groups were assessed using one-way ANOVA with LSD post-hoc test.

of MGO-challenged COCs with the TAB cocktail reversed the decreases observed in both MMI ( $8.94 \pm 0.19\%$  vs.  $9.47 \pm 0.42\%$ ) and MMP ( $2.01 \pm 0.45\%$  vs.  $1.74 \pm 0.08\%$ ) to levels similar to those of the control group ( $P > 0.05$ ).

#### The effect of co-treatment of MGO-challenged COCs with TAB cocktail during IVM on the mRNA expression of *Cbs*, *Cse*, and *Rage* in cumulus cells

In matured oocytes, mRNA expression of *Cbs* and *Cse* genes was not observed. However, in cumulus cells, exposure to MGO during IVM significantly decreased *Cbs* mRNA expression (Fig. 6A,  $P < 0.05$ ) but did not affect *Cse* mRNA expression (Fig. 6B,  $P > 0.05$ ). Interestingly, supplementation of COCs with the TAB cocktail during IVM did not alter the mRNA expression of either *Cbs* (Fig. 6A,  $P > 0.05$ ) or *Cse* (Fig. 6B,  $P > 0.05$ ) compared to standard culture conditions. Furthermore, co-treatment of MGO-challenged COCs with the TAB cocktail significantly increased the mRNA expression of both *Cbs* (Fig. 6A,  $P < 0.05$ ) and *Cse* (Fig. 6B,  $P < 0.05$ ), indicating a potential protective effect against MGO-induced suppression.

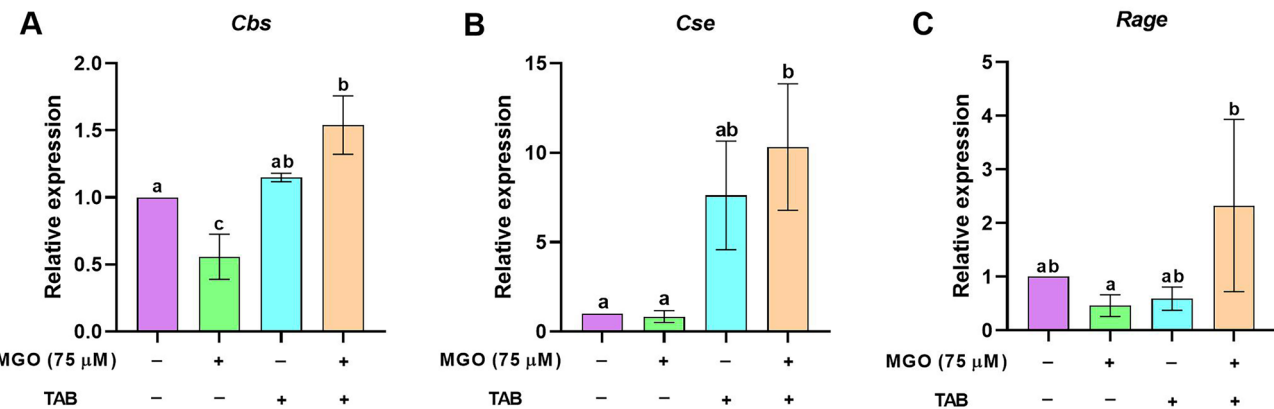


**Figure 6.** The effect of co-treatment of MGO-challenged COCs with TAB cocktail during IVM on the mRNA expression of (A) *Cbs*, (B) *Cse*, and (C) *Rage* in cumulus cells. The relative mRNA expression of (A) *Cbs*, (B) *Cse*, and (C) *Rage* in cumulus cells in various treatment groups. Three replicates were included. Data are presented as means  $\pm$  SEM. Different letters (a, b, and c) indicate significant differences between the treatment groups at  $P < 0.05$ . Statistical differences between groups were assessed using one-way ANOVA with LSD post-hoc test.

Regarding *Rage* expression, neither MGO treatment nor TAB cocktail supplementation during IVM had a significant effect on *Rage* mRNA expression in cumulus cells compared to standard culture conditions (Fig. 6C,  $P > 0.05$ ). However, co-treatment of MGO-challenged COCs with the TAB cocktail showed a trend towards increased *Rage* mRNA expression (Fig. 6C,  $P > 0.05$ ) compared to MGO-challenged COCs alone.

#### Effects of MGO during IVM in denuded oocytes

Immature DOs were cultured with various concentrations of MGO (20, 40, 75, and 150  $\mu$ M) alongside a control group. After 18 h, maturation rates were assessed. As shown in Fig. 7A, maturation rates significantly decreased with 75  $\mu$ M ( $44.17 \pm 5.12\%$ ) and 150  $\mu$ M ( $11.69 \pm 1.94\%$ ) MGO compared to other groups ( $P < 0.05$ ). Moreover, the maturation rate with 150  $\mu$ M MGO was lower than with 75  $\mu$ M MGO ( $P < 0.05$ ).

Subsequent assessment of fertilization rates (Fig. 7B) revealed a significant decrease in DOs matured with 75  $\mu$ M ( $20.78 \pm 3.82\%$ ) and 150  $\mu$ M ( $2.13 \pm 0.76\%$ ) MGO compared to other groups ( $P < 0.05$ ). The formation of 2PN (pronucleus) was significantly lower with 150  $\mu$ M MGO compared to 75  $\mu$ M MGO (Fig. 7B,  $P < 0.05$ ). Regarding blastocyst formation rates (Fig. 7C), groups exposed to 40, 75, and 150  $\mu$ M MGO showed similar rates ( $6.19 \pm 0.63\%$ ,  $4.23 \pm 1.91\%$ , and  $0.0 \pm 0.0\%$ , respectively), which were significantly lower than the control ( $26.17 \pm 5.24\%$ ) and 20  $\mu$ M MGO ( $18.70 \pm 3.61\%$ ) groups ( $P < 0.05$ ). Based on these findings, concentrations of 40 and 75  $\mu$ M MGO were selected for further analysis.

It's noteworthy that while 40  $\mu$ M MGO during IVM did not significantly reduce blastocyst rates in matured cumulus-oocyte complexes (COCs) compared to the control group ( $P > 0.05$ ) (Fig. 7C), this concentration significantly decreased blastocyst rates in DOs compared to the control group ( $P < 0.05$ ), similar to the levels observed with 75 and 150  $\mu$ M MGO ( $P > 0.05$ ) (Fig. 7C). These results underscore the crucial role of cumulus cells in supporting oocyte quality and developmental competence during IVM.

#### The addition of the TAB cocktail does not improve the developmental competence of DOs that were exposed to MGO stress

We detected the mRNA expression of *Cbs* and *Cse* only in cumulus cells not in matured oocytes, suggesting that oocytes may be more vulnerable to oxidative damage without the protective role of cumulus cells. CBS and CSE are crucial enzymes in the transsulfuration pathway, responsible for converting methionine to cysteine and maintaining cellular antioxidant defense and redox balance. To investigate the potential protective role of TAB cocktail in DOs exposed to MGO stress, we co-treated immature DOs with MGO and TAB. Contrary to our hypothesis, co-treatment of DOs with MGO stress (75  $\mu$ M) and the TAB cocktail did not ameliorate the decreased level of maturation and 2PN formation rates compared to the group treated with 75  $\mu$ M MGO alone (Fig. 7D,E,  $P > 0.05$ ). Furthermore, the TAB cocktail did not improve the decreased blastocyst formation rates in DOs challenged with 40 and 75  $\mu$ M MGO (Fig. 7F,  $P > 0.05$ ). These findings suggest that cumulus cells are essential for the protective effects of TAB in oocytes exposed to MGO-induced stress.

In summary, while cumulus cells play a critical role in protecting oocytes under oxidative stress, the TAB cocktail did not demonstrate significant protective effects in this experimental context. Further research is warranted to understand the mechanisms underlying these observations and to explore alternative strategies to enhance oocyte resilience to oxidative stress during in vitro maturation.

#### The addition of a TAB cocktail does not modulate the redox balance in DOs that were exposed to MGO stress

To investigate whether the impaired redox state in matured DOs exposed to MGO (75  $\mu$ M) could be restored using a TAB cocktail, we conducted co-treatment during IVM. Contrary to expectations, TAB did not restore

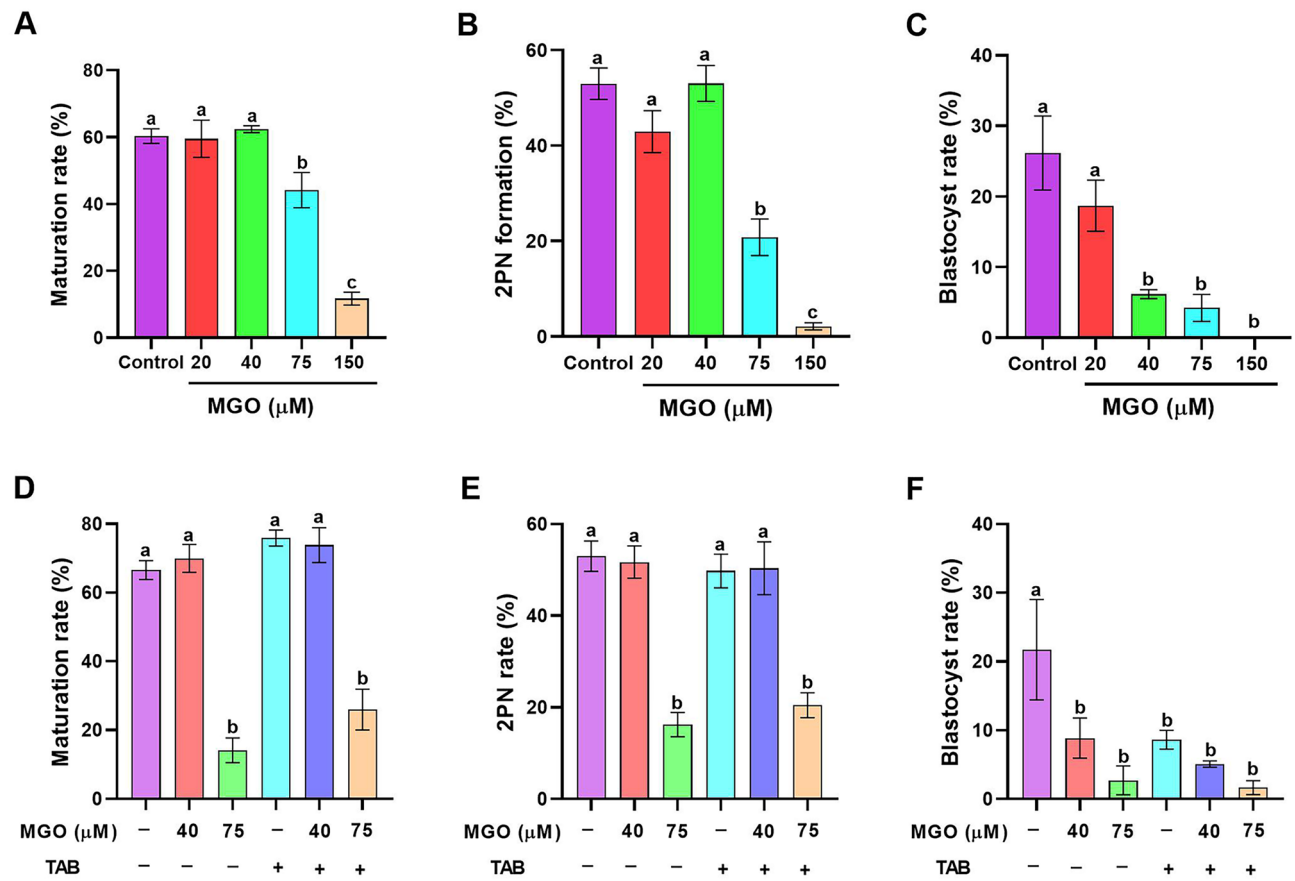


**Figure 7.** IVM medium supplementation with TAB cocktail does not improve the developmental competence of MGO-challenged DOs. DOs were cultured in IVM medium with indicated concentrations of MGO (20, 40, 75 and 150  $\mu\text{M}$ ) for 16–18 h and then IVF was carried out on matured DOs and then cultured in G-TL medium for 4.5 days; (A) Maturation rate/ GV, (B) 2PN formation rate/ GV (C) Blastocyst rate/ GV; DOs were cultured in IVM medium in presence of MGO (40 or 75  $\mu\text{M}$ ) and/or TAB (Taurine: 10 mM; ALA: 10  $\mu\text{M}$ ; B6: 10  $\mu\text{M}$ ) for 16–18 h and then IVF was carried out on matured DOs and then cultured in G-TL medium for 4.5 days; (D) Maturation rate/ GV, (E) 2PN formation rate/ GV (F) Blastocyst rate/ GV; At least 50 DOs were cultured in each replicate of each treatment group. Five replicates were included. Data are presented as mean  $\pm$  SEM. Different letters (a, b, and c) indicate significant differences between the treatment groups at  $P < 0.05$ . Statistical differences between groups were assessed using one-way ANOVA with LSD post-hoc test.

ROS levels to those observed in the standard culture medium ( $23.90 \pm 1.28$  vs  $16.57 \pm 1.04$ ; Fig. 8A,B). Moreover, TAB exacerbated the reduction in GSH caused by MGO ( $33.31 \pm 1.12$  vs.  $50.39 \pm 2.99$ ;  $P < 0.05$ , Fig. 8C,D).

## Discussion

Elevated levels of MGO and Amadori products, resulting from the Maillard reaction, can originate from both endogenous and exogenous sources. Numerous studies have demonstrated that metabolic disorder such as obesity, PCOS, and diabetes contribute to an endogenous increase in MGO and/or AGEs. These conditions are known to adversely affect a woman's entire fertility journey<sup>25,26</sup>.

Research indicates that heightened levels of MGO and/or AGEs can detrimentally impact reproductive health, spanning from preconception to postpartum stages. Mechanistic studies have shown that AGEs induce inflammation and oxidative stress in the reproductive system. Therefore, understanding these mechanisms is crucial, and targeted interventions are being developed to mitigate these effects. However, further research is needed to fully elucidate the biochemical pathways through which MGO and AGEs influence reproductive health. Future studies should explore specific mechanisms and consider physiological interventions aimed at mitigating the adverse effects of MGO and AGEs on fertility and reproductive outcomes.

During this study, we investigated the impact of 75  $\mu\text{M}$  MGO exposure on COCs during IVM, focusing on developmental outcomes such as maturation rates, 2PN formation, and blastocyst development. Our results indicate a significant deterioration in these developmental parameters, consistent with previous research. Emidio et al. demonstrated reduced rates of MII oocytes in mice exposed to similar concentrations of MGO<sup>9</sup>. Similarly, Liu et al. found impaired polar body extrusion under comparable conditions<sup>10</sup>. Furthermore, Tatone et al. linked MGO exposure to meiotic abnormalities, including spindle aberrations and chromosome congression failure<sup>11</sup>. Chan et al. reported detrimental effects of lower concentrations (5–10  $\mu\text{M}$ ) of MGO on mouse oocyte maturation,

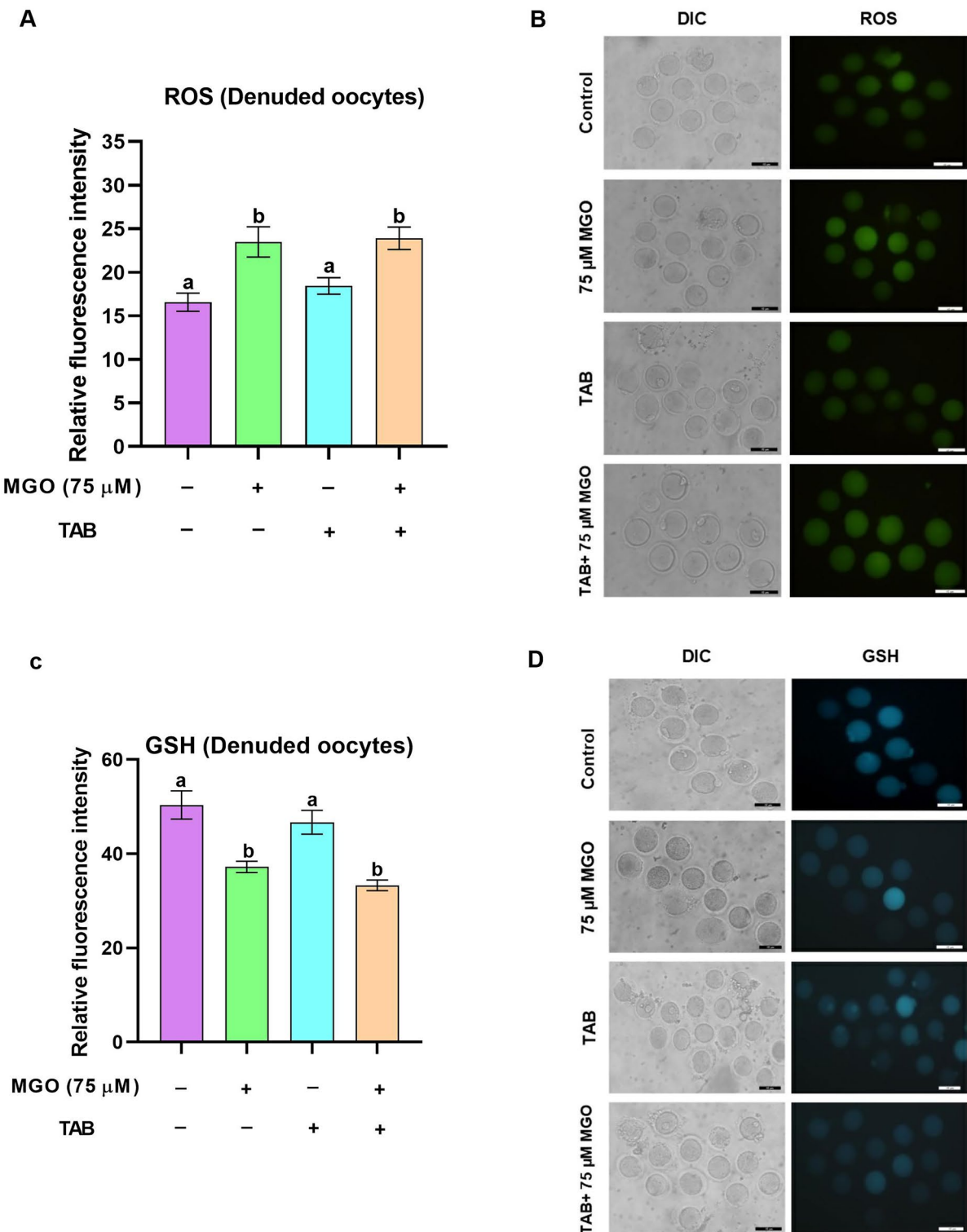


**Figure 8.** The addition of the TAB cocktail does not modulate the redox balance in MGO-challenged DOs. The relative fluorescence intensity of (A) ROS and (C) GSH levels in matured oocytes, (B) The representative images show the ROS levels, and (D) GSH levels using a fluorescence microscope. Number of stained oocytes was 20 in each replicate of each treatment group. Five replicates were included. The scale bars represent 50  $\mu$ m. Data are presented as means  $\pm$  SEM. Different letters (a and b) indicate significant differences between the treatment groups at  $P < 0.05$ . Statistical differences between groups were assessed using one-way ANOVA with LSD post-hoc test.

fertilization, and pre-implantation embryo development<sup>6</sup>. Furthermore, they noticed that treatment of oocytes with MGO during IVM increased the post-implantation resorption and decreased the fetal weight, confirming the reduced number of ICM and TE in derived blastocysts<sup>6</sup>. Hutchison et al. noted that 8 μM AGEs in culture medium did not affect blastocyst rates but significantly reduced hatching rate and also TCN and TE cell numbers within blastocysts<sup>27</sup>. The discrepancies in the MGO concentrations used in the mentioned studies may be attributed to variations in the animal strains tested and/or in the sources of MGO/AGEs substance employed.

To elucidate the mechanisms underlying these observations, we examined the impact of MGO on redox balance within COCs. Our study revealed disruptions in ROS and GSH levels, indicating oxidative stress induction by MGO, consistent with previous reports on the reproductive system<sup>1</sup>.

The glyoxalase system, mediated by GLO1 and GLO2 enzymes, converts MGO into D-lactate via S-D-lactoyl-glutathione, a process occurring on the cytosol of mammalian cells. This enzymatic activity is pivotal as MGO can sequester GSH, diminishing cellular antioxidant defenses and disturbing redox balance, consequently elevating ROS levels<sup>28</sup>. Moreover, MGO's reactivity facilitates the formation of AGEs, which in turn activates NADPH oxidase enzymes, further exacerbating ROS production<sup>28</sup>. Additionally, MGO could modify the expression of certain enzymes, such as superoxide dismutase (SOD), glutathione peroxidases (GPx), glutathione transferases (GT), Nrf2, and NF-κB<sup>29–32</sup>, leading to increased ROS production. Our unpublished data from studies on COCs during IVM indicate that MGO exposure decreases mRNA expression of *Nrf2* and *NF-κB* within COCs, potentially compromising their redox state. Additionally, MGO disrupts mitochondrial function in matured COCs, exacerbating ROS production. In the current study, as we have mentioned earlier, we found that MGO disrupted both MMI and MMP in matured COCs which can be another possible explanation for the impaired redox state in MGO-challenged COCs.

While the direct relationship between AGEs and H<sub>2</sub>S production remains unclear, emerging researches suggest that H<sub>2</sub>S possesses cytoprotective properties against AGEs-induced damage. H<sub>2</sub>S acts as an antioxidant and anti-inflammatory agent, mitigating oxidative stress associated with AGEs accumulation<sup>12,33</sup>.

A growing body of evidence has suggested that H<sub>2</sub>S has wide regulatory effects in biological systems<sup>34</sup>. Especially, its roles in diabetes have attracted more and more attention. Yang and colleagues showed that H<sub>2</sub>S protected HaCaT skin cells against MGO-induced dysfunctions<sup>35</sup>. In addition, Zhang and colleagues found that the exposure of RSC96 cells to both high glucose and MGO downregulated CBS expression and reduced the ability of cells to produce H<sub>2</sub>S<sup>36</sup>. The authors concluded that the deficiency of CBS/H<sub>2</sub>S may be one of the most important reasons for the induced injury by MGO, which is consistent with the fact that the levels of H<sub>2</sub>S are reduced in the plasma of diabetic patients<sup>37</sup>. Consistent with these findings, our study observed reduced *Cbs* mRNA expression in MGO-exposed COCs during IVM, potentially contributing to compromised redox balance and oocyte quality. As previously mentioned, both CBS and CSE enzymes play a crucial role in the synthesis of H<sub>2</sub>S in the transsulfuration pathway. Numerous studies have demonstrated the cytoprotective properties of H<sub>2</sub>S in various cell lines under in vitro conditions, attributed to its ability to counteract superoxide anions<sup>38,39</sup>, neutralize free radicals such as peroxynitrite<sup>40</sup>, and mitigate other ROS in vitro<sup>41</sup>. Despite not directly measuring H<sub>2</sub>S levels, our findings suggest that decreased mRNA expression of *Cbs* and *Cse* in COCs exposed to MGO likely reduces H<sub>2</sub>S production, impairing antioxidant defenses and exacerbating oxidative stress. This highlights the critical role of H<sub>2</sub>S in maintaining redox balance and protecting against oxidative damage in oocytes.

In this study, we observed reduced mRNA expression levels of *Cbs* and an impaired redox state characterized by decreased GSH levels and increased ROS levels, in MGO-challenged COCs. To mitigate these adverse effects, we supplemented the maturation medium with a TAB cocktail. This cocktail was formulated based on prior researches<sup>12,16,20,42</sup> indicating that dicarbonyl compound compromise the transsulfuration pathway and reduce antioxidant capacity.

R-α-lipoic acid (ALA) is known for its role as a cofactor in mitochondrial respiratory enzymes and its ability to inhibit protein glycation and AGEs formation, effects observed both in vitro and in vivo<sup>20,42</sup>. In our formulation of the TAB cocktail, we used 10 μM ALA in the cocktail to enhance antioxidant capacity and mitigate oxidative stress associated with MGO exposure. ALA promotes GSH synthesis by facilitating the conversion of cystine to cysteine, a critical precursor of GSH, thereby maintaining cellular redox balance and protecting against oxidative damage<sup>21</sup>. Additionally, ALA has been shown to increase H<sub>2</sub>S levels and enhance the expression of CSE, an enzyme involved in H<sub>2</sub>S production, suggesting potential roles in modulating H<sub>2</sub>S signaling and cellular functions<sup>22</sup>.

In formulating our TAB supplement, we hypothesized that direct supplementation with cysteine, rather than taurine, to the IVM medium, might more effectively elevate cellular cysteine levels and thereby increase GSH production<sup>16</sup>. Excess cysteine, however, may be metabolized by cysteine dioxygenase (CDO) into hypotaurine and further oxidized to taurine. Additionally, previous studies speculate that an excess amount of taurine could have negative feedback on CDO expression and/or activity<sup>16,17</sup>. Previous studies suggest that a combination of cysteine and taurine supplementation could synergistically elevate free cysteine levels and increase circulating H<sub>2</sub>S, possibly through regulatory feedback mechanism<sup>16</sup>.

Taurine, a non-proteogenic amino acid and a terminal metabolite in mammals, plays a crucial role in various vital cellular functions and redox regulation across tissues<sup>43</sup>. Recent studies highlight its potential to mitigate oxidative stress. For instance, Xu and colleagues demonstrated that pre-treatment of porcine mammary epithelial cells (PMECs) with taurine enhanced cell viability, increased superoxide dismutase activity, and reduced intracellular ROS levels following H<sub>2</sub>O<sub>2</sub> exposure, indicating its protective role against oxidative damage<sup>44</sup>. Moreover, taurine is recognized for its anti-glycation properties, effectively inhibiting in vitro glycation and reducing the accumulation of AGEs. These properties suggest that taurine supplementation may offer therapeutic benefits in managing complications associated with diabetes, including improved glycemic control and reduced AGEs formation. Studies have also reported significant reductions in MGO and pentosidine levels in patients with Type 2 diabetes mellitus (T2DM) following taurine supplementation, underscoring its potential clinical relevance<sup>45,46</sup>.

Vitamin B6 plays a crucial role as a cofactor for CBS and CSE enzymes in the transsulfuration pathway, a process essential for the conversion of homocysteine into cysteine and the regulation of endogenous H<sub>2</sub>S production<sup>16</sup>. Additionally, vitamin B6 is involved in approximately 150 reactions that influence the metabolism of glucose, lipids, amino acids, DNA, and neurotransmitters. Researches indicate that pyridoxamine (PM), a form of vitamin B6, inhibits the post-Amadori steps of the Maillard reaction by sequestering catalytic metal ions and preventing the oxidative degradation of Amadori intermediate<sup>47</sup>. PM also scavenges toxic carbonyl products resulting from sugar and lipid degradation and inhibits ROS<sup>48–51</sup>. Furthermore, studies have demonstrated that pyridoxal 5'-phosphate (PLP), the active form of vitamin B6, also inhibits post-Amadori reactions and, thereby reducing the formation of AGEs<sup>52,53</sup>. These findings collectively suggest that vitamin B6 supplementation could be a promising strategy for inhibiting AGEs formation and mitigating oxidative stress, offering potential therapeutic benefits in conditions where these processes are implicated.

In line with studies introducing taurine, alpha lipoic acid, and vitamin B6 as potent anti-AGEs and anti-oxidant agents, we formulated a TAB cocktail to counteract the challenges posed by MGO during the *in vitro* maturation process. Our study demonstrated that while supplementation of the maturation medium with TAB did not affect normal embryo development it successfully mitigated the negative effects of MGO on the developmental competence of challenged COCs, including maturation, 2PN, and blastocyst rates. These results underscore the protective effect of TAB against MGO-induced damage to COCs. Supporting our results, DI Emidio et al. showed that supplementing the IVM medium with 2 μM resveratrol, an antioxidant and SIRT1 activator, improved the maturation rate of MGO-challenged COCs exposed to 75 μM MGO<sup>9</sup>. Similarly, Liu et al. reported that resveratrol supplementation (5, 10, and 25 μM) increased polar body extrusion in MGO-challenged COCs. Furthermore, our assessment of derived blastocysts revealed that TAB restored impaired cell lineage allocation in blastocysts developed from COCs exposed to MGO stress. Contrary to our results, Hutchison and colleagues found that neither metformin nor a cocktail of antioxidants including N-acetyl-l-cysteine, N-acetyl-l-carnitine, and α-lipoic acid, improved embryo outcomes, as assessed by total cell number and TE/ICM cell number, in the presence of 8 μmol/L AGEs<sup>27</sup>.

Oocytes and embryos are highly sensitive to micro-environmental variables such as dicarbonyl and oxidative stresses. We hypothesized that using additional anti-AGEs and anti-oxidants, such as the TAB cocktail, during MGO challenges might improve the efficiency of IVM and IVF processes (21, 34, 35, 36 + MGO/AGEs). In this study, we showed that supplementing the IVM medium with the TAB cocktail elevated GSH levels, mitochondrial mass, and mitochondrial membrane potential in MGO-challenged COCs. Additionally, TAB reduced ROS levels to normal level. Supporting our findings, Liu et al. demonstrated that supplementation of the maturation medium with various concentrations of resveratrol (5, 10, and 25 μM) scavenged ROS induced by MGO (75 μM) in mouse oocytes. Furthermore, they showed that resveratrol improved the diminished mitochondrial function by MGO<sup>10</sup>.

As mentioned earlier, CBS and CSE are two crucial enzymes in the transsulfuration pathway. Previous studies have shown that CBS and CSE are exclusively expressed in cumulus cells<sup>47,49</sup>. Consistent with these findings, we detected mRNA expression of *Cbs* and *Cse* only in cumulus cells not in matured oocytes. However, a recent study demonstrated the expression of CBS in mouse oocytes<sup>54</sup>. We hypothesized that the TAB cocktail might exert its anti-AGEs and antioxidant effects through the transsulfuration pathway by enhancing the activity of CBS and CSE. To test this hypothesis, we designed an experiment to explore the supportive role of the TAB cocktail in DOs. Interestingly, we observed that the TAB cocktail did not improve the diminished developmental competence (maturation, 2PN, and blastocyst rates) or the quality (ROS and GSH levels) of MGO-challenged DOs. In line with our results, Tatone et al. showed that DO oocytes exposed to 150 and 300 mM MGO exhibited a significantly lower percentage of polar body emission compared to COCs<sup>18</sup>. This suggests that, in addition to the active transsulfuration pathway in cumulus cells due to the presence of CBS and CSE, cumulus cells may also protect the oocyte from oxidative stress during maturation through their antioxidant role, which warrants further exploration<sup>55,56</sup>.

## Conclusion

In conclusion, this study demonstrated that exposure to MGO during IVM significantly reduced the maturation rate, 2PN rate, blastocyst rate, and embryo quality. MGO-induced oxidative stress disrupted the redox balance, increased ROS levels, decreased GSH levels, and impaired mitochondrial function within COCs, highlighting the critical equilibrium required for proper COCs function. The formulation of a TAB cocktail presents a novel approach to mitigate these MGO-induced disruptions. By reinforcing the transsulfuration pathway and enhancing antioxidant capacity, the TAB cocktail aimed to restore redox balance and improve developmental competence in MGO-challenged oocytes. Our findings shed light on the intricate mechanisms underlying MGO-induced impairments and offer a promising approach for intervention through the TAB cocktail. As we navigate the challenges posed by MGO and its implications for fertility, further research is essential to fully understand its effects and develop targeted strategies to protect reproductive well-being. Future studies should focus on elucidating the detailed mechanisms by which the TAB cocktail exerts its protective effects and exploring its potential in clinical applications to enhance fertility outcomes.

## Material and methods

### Ethics

This study is in accordance with the ARRIVE guidelines 2.0. All animal care and procedures were approved by the Institutional Ethical Committee of the Royan Institute (IR.ACECR.AEC.1401.069). In addition, all methods used in the current study were carried out under the Institutional Review Board and Institutional Ethical Committee of the Royan Institute guidelines and regulations.

## Animals

In this study, nine-week-old female and twelve-week-old male NMRI mice were obtained from Royan Institute (Isfahan, Iran). The schedule in the animal house includes ad libitum access to food and water, temperature  $21 \pm 2$  °C, humidity  $50 \pm 10\%$ , and 12 h light and 12 h dark. For euthanasia, the mice were initially anesthetized through an intraperitoneal injection of ketamine (80 mg/kg) and xylazine (5 mg/kg). Once deep anesthesia was confirmed, cervical dislocation was carried out by firmly holding the mouse at the base of the tail and the back of the neck, swiftly extending the neck to dislocate the cervical vertebrae. Subsequently, death was verified by the cessation of breathing and the absence of a heartbeat.

## Chemicals

Unless otherwise mentioned, all materials and media in this study were obtained from Sigma-Aldrich Company (St Louis, MO, USA) and Gibco (Life Technologies, Rockville, MD, USA), respectively.

## Preparation of MGO solution and TAB cocktail

A 500 mM stock solution of methylglyoxal (M0252; Sigma) was prepared and stored at 4 °C. This stock solution was diluted using α-MEM to obtain the desired final concentrations of 20, 40, 75, and 150 μM, based on previous studies<sup>5,9–11</sup>. The TAB cocktail consisted of 10 μM R-α-lipoic acid (T1395, Sigma), 10 μM vitamin B6 (P9255, sigma), and 10 mM Taurine (T0625, Sigma). The optimal concentrations for TAB were according to previous studies<sup>21,23,24</sup>. Commercially available ALA, B6, and taurine were formulated into stock solutions at concentrations of 100, 200, and 400 mM, respectively. These stock solutions were then used to prepare the TAB cocktail for use in the experiments. All stock solutions were stored under appropriate conditions to ensure stability and efficacy until use.

## Mice Superovulation and oocyte collection

Female mice were superovulated with an intraperitoneal injection of 10 IU pregnant mare's serum gonadotropin (PMSG) (Pregnocol, Armidale, Australia). Forty-eight h post-PMSG administration, the mice were sacrificed, and both ovaries were removed. Visible antral follicles on the ovarian surface were gently punctured to collect COCs and DOs. Both COCs and DOs were collected in Hepes-buffered tissue culture medium 199 (HTCM-199) supplemented with 10% fetal bovine serum (FBS). The collected COCs and DOs were then cultured in the maturation medium.

## IVM and treatment with different concentrations of MGO and TAB

Ten COCs or DOs were transferred into a 20 μl droplet of maturation medium (α-MEM supplemented with 50 μg/ml Streptomycin, 75 IU/ml Penicillin G, 5% FBS, and 100 mIU/ml recombinant human FSH and 7.5 IU/ml HCG) containing the indicated supplementations. The COCs and DOs were cultured for 16–18 h in a 6% CO<sub>2</sub> incubator at 37 °C. After IVM, the COCs from each group were treated with 50 IU/ml ovine hyaluronidase and gently pipetted to removal all cumulus cells. The matured oocytes, free of cumulus cells, were collected from COCs or DOs and used for further assessments.

## IVF

Approximately 16 h after IVM of mouse COCs, the cauda epididymis of a sacrificed male mouse was dissected out. The epididymis was squeezed using a 16-gauge needle and incubated in sperm activation medium for 45 min at 37 °C. After sperm activation, groups of 10 COCs or DOs were transferred into 20 μl drops of fertilization medium. To each drop, 10 μl of sperm suspension was added. Four to six hours after in vitro insemination, cumulus cells were removed mechanically by pipetting. Zygotes with two defined male and female pronuclei (2PN) were washed and transferred to G-TL™ medium (G-series sequential medium, Vitrolife, 10,145). 2PN embryos in groups of 6 were cultured in 30 μl drops of G-TL™ medium and incubated for approximately 4.5 days until reaching the blastocyst stage.

## Differential staining

The quality of derived blastocysts at day 4.5 was assessed in terms of the blastomere allocation to inner cell mass (ICM), trophectoderm cells (TE), and total cell number (TCN) using differential staining. Briefly, blastocysts were washed in basic medium (HTCM-199 supplemented with 5 mg/mL BSA). After washing, they were transferred to 0.5% Triton X-100 (T8787) for 30 s (s). The blastocysts were then incubated in 30 mg/mL of propidium iodide (P4170) for 20 s. Subsequently, the blastocysts were stained with ice-cold ethanol containing 10 mg/mL Hoechst 33,342 (H33342) for 15 min. Stained blastocysts were mounted in a drop of mounting solution. The samples were observed under a fluorescence microscope (Olympus, Tokyo, Japan). ICM and TE cells were distinguished based on their blue and red colors, respectively<sup>21</sup>.

## Measurement of intracellular ROS

The maturation medium, as previously described, was supplemented with 10 μM of DCF (2',7'-dichlorofluorescein, Sigma D6883) and used for 1 h at 37 °C in a humidified atmosphere of 5% CO<sub>2</sub> in air. After incubation, the live oocytes were washed with base medium<sup>21</sup>. The stained live oocytes were then placed in a plate covered with mineral oil containing a drop of PBS supplemented with 1 mg/mL polyvinyl alcohol (PVA, P8136). The oocytes were exposed to UV light using a fluorescent microscope (Olympus, IX71, Japan). Fluorescence intensity was captured with a DP-72 camera (Olympus, Japan) and measured using Image J software (National Institute Mental, health, Bethesda, MD, USA).

### Measurement of intracellular GSH

The staining process for oocytes included the following three steps, a) oocytes were incubated in PBS<sup>-</sup> + 1 mg/mL PVA supplemented with 10 µM cell tracker blue (Cell tracker™ blue CMF2HC, Molecular Probes, Eugene, OR, USA) for 30 min at 37° C in a humidified atmosphere of 5% CO<sub>2</sub> in air; b) After incubation, The oocytes were observed under a fluorescent microscope (Olympus, IX71, Japan) equipped with UV filters. The oocytes were placed in a drop of PBS<sup>-</sup> + 1 mg/mL PVA for observation. The fluorescence intensity of each oocyte was analyzed by Image J software. (National Institutes of Health, Bethesda, MD, USA).

### Measurement of mitochondrial mass

Live oocytes were incubated in PBS<sup>-</sup> supplemented with 1 mg/mL PVA containing 400 nM Mitotracker Green<sup>FM</sup> (Mito-Tracker Green<sup>FM</sup>, Invitrogen, Molecular Probes, Eugene, OR, USA) for 30 min at 37 °C<sup>57</sup>. After incubation, the oocytes were washed with PBS to remove excess dye. The fluorescence intensities of the oocytes were then analyzed using ImageJ software (National Institutes of Health, Bethesda, MD, USA).

### Measurement of mitochondrial membrane potential

The mitochondrial membrane potential was determined using the mitochondrial membrane potential assay kit with JC1 (JC-1 fluorochrome; Cat. No. M34152; Invitrogen, Carlsbad, CA). Briefly, oocytes were stained with PBS<sup>-</sup> supplemented with 1 mg/mL PVA containing 20 µM JC1 for 30 min. After staining, the live oocytes were placed in PBS<sup>-</sup> + 1 mg/mL PVA for imaging<sup>57</sup>. The fluorescence intensity of JC1 aggregates and monomers was determined using a fluorescence microscope (Olympus, IX71, Japan). Fluorescence intensities were measured using ImageJ software (National Institutes of Health, Bethesda, MD, USA), ensuring the measurement area was kept as consistent as possible to minimize technical error. The ratio of aggregates and monomers was calculated as the average intensity of aggregates divided by the average intensity of monomers. The JC1 assay was performed in triplicate.

### Evaluation of mRNA expression

The mRNA expression of *Cbs*, *Cse*, and *Rage* genes within cumulus cells and oocytes were subjected to examination via real-time reverse transcription polymerase chain reaction (RT-PCR). Cumulus cells, derived from a pool of 80 matured oocytes, each encompassing approximately 105, underwent meticulous RNA extraction. The protocol prescribed by the manufacturer of the RNeasy Micro Kit (QIAGEN, Germany, 74,004) was assiduously adhered to for each replication, culminating in the acquisition of total RNA from 80 matured oocytes in each repetition. This intricate process was repeated three times to ensure robust biological validity.

The extracted RNA underwent a transformative metamorphosis through reverse transcription, a feat accomplished by the proficient deployment of a cDNA Synthesis kit (Biotechrabbit, Germany, BR0400403) in strict adherence to the manufacturer's directives. The quality and integrity of the resultant cDNA underwent rigorous scrutiny through the prism of PCR, facilitated by housekeeping primer β-actin, enlisted as a reference gene in the RT-PCR analysis. For each specimen, a trio of technical replicates was meticulously executed, and the mean cycle threshold (Ct) was computed at 62. Relative expression values were derived through the normalization of Ct values to β-actin, serving as the benchmark. The fold change in gene expression was ascertained through the calculated 2-ΔCT. The primer selection process was executed with precision through the utilization of the Primer 3 program (<http://primer3.ut.ee>), and the salient characteristics of these primers are duly cataloged in the supplementary information (Table S1).

The mRNA expression of *Cbs*, *Cse*, and *Rage* genes in cumulus cells and *Cbs* and *Cse* in oocytes were analyzed using real-time reverse transcription polymerase chain reaction (RT-PCR) in cumulus cells. The total RNA of cumulus cells derived from 80 matured oocytes (~10<sup>5</sup>) and the total RNA of 80 matured oocytes in each replicate were extracted using RNeasy Micro Kit (QIAGEN, Germany, 74,004) for each replicate according to the manufacturer's protocol. Three independent biological repetitions were carried out. Total RNA was reverse transcribed using a cDNA Synthesis kit (Biotechrabbit, Germany, BR0400403) according to the manufacturer's protocol. Quality and integrity of cDNA was checked using PCR and housekeeping primer (*β-actin*), as a reference gene in the RT-PCR analyses. Three technical replicates were performed for each sample and the mean cycle threshold (Ct) was calculated<sup>57</sup>. Relative expression was computed using Ct values that were normalized against *β-actin*. Fold change in gene expression was calculated using 2-ΔCT. All the primers were designed by the Primer 3 program ((<http://primer3.ut.ee/>)) and their characteristics are listed in supplementary information (Table S1).

### Statistical data analysis

All assessments were carried out at least three times. Data are presented as mean ± standard error of the mean (SEM). One-way analyses of variance (ANOVA) were applied in the SPSS program (v.23, NY, USA) to compare the effect of the treatments between various groups ( $\alpha=0.05$ ), followed by the LSD post-hoc test. Statistical significance was set at  $P<0.05$ . Graphs created by GraphPad Prism (v.6.0.1).

### Data availability

The datasets used and/or analyzed during the current study are available from the corresponding author upon reasonable request.

Received: 23 December 2023; Accepted: 3 July 2024

Published online: 02 August 2024

## References

1. Merhi, Z. Advanced glycation end products and their relevance in female reproduction. *Hum. Reprod.* **29**, 135–145 (2014).
2. Gkogkolou, P. & Böhm, M. Advanced glycation end products: key players in skin aging?. *Derm.-Endocrinol.* **4**, 259–270 (2012).
3. Teodorowicz, M., Hendriks, W. H., Wicher, H. J. & Savelkoul, H. F. Immunomodulation by processed animal feed: The role of maillard reaction products and advanced glycation end-products (AGEs). *Front. immunol.* **9**, 2088 (2018).
4. Sun, Q. *et al.* Endogenous hydrogen sulfide promotes human preimplantation embryonic development by regulating metabolism-related gene expression. *Nitric Oxide.* **120**, 9–15 (2022).
5. Hsuuw, Y. D. *et al.* Curcumin prevents methylglyoxal-induced oxidative stress and apoptosis in mouse embryonic stem cells and blastocysts. *J. Cell. Physiol.* **205**, 379–386 (2005).
6. Chang, Y. J. & Chan, W. H. Methylglyoxal has injurious effects on maturation of mouse oocytes, fertilization, and fetal development, via apoptosis. *Toxicol. Lett.* **193**, 217–223 (2010).
7. Ambroggio, J. D., Casson, P. & Merhi, Z. Soluble receptor for advanced glycation end-products (sRAGE): a potential indicator of ovarian response to controlled ovarian hyperstimulation. *Fertil. Steril.* **100**, S136 (2013).
8. Jinno, M. *et al.* Advanced glycation end-products accumulation compromises embryonic development and achievement of pregnancy by assisted reproductive technology. *Hum. Reprod.* **26**, 604–610 (2011).
9. Di Emidio, G. *et al.* SIRT1 participates in the response to methylglyoxal-dependent glycative stress in mouse oocytes and ovary. *Biochim. Biophys. Acta. Mol. Basis. Dis.* **1865**, 1389–1401 (2019).
10. Liu, Y. *et al.* Resveratrol protects mouse oocytes from methylglyoxal-induced oxidative damage. *PLoS one.* **8**, e77960 (2013).
11. Tatone, C. *et al.* Evidence that carbonyl stress by methylglyoxal exposure induces DNA damage and spindle aberrations, affects mitochondrial integrity in mammalian oocytes and contributes to oocyte aging. *Hum. Reprod.* **26**, 1843–1859 (2011).
12. Chang, T., Untereiner, A., Liu, J. & Wu, L. Interaction of methylglyoxal and hydrogen sulfide in rat vascular smooth muscle cells. *Antioxid. Redox. Signal.* **12**, 1093–1100 (2010).
13. Altaany, Z., Yang, G. & Wang, R. Crosstalk between hydrogen sulfide and nitric oxide in endothelial cells. *J. Cell. Mol. Med.* **17**, 879–888 (2013).
14. Ning, N. *et al.* Dysregulation of hydrogen sulphide metabolism impairs oviductal transport of embryos. *Nat. Commun.* **5**, 4107 (2014).
15. Krejcova, T. *et al.* Hydrogen sulfide donor protects porcine oocytes against aging and improves the developmental potential of aged porcine oocytes. *PLoS One.* **10**, e0116964 (2015).
16. Dattilo, M., Fontanarosa, C., Spinelli, M., Bini, V. & Amoresano, A. Modulation of human hydrogen sulfide Metabolism by Micro-nutrients, preliminary Data. *Nutr. Metab. Insights.* **15**, 11786388211065372 (2022).
17. Sun, Q. *et al.* Taurine supplementation lowers blood pressure and improves vascular function in prehypertension: randomized, double-blind, placebo-controlled study. *Hypertension.* **67**, 541–549 (2016).
18. Zhou, H. *et al.* Hydrogen sulfide reduces RAGE toxicity through inhibition of its dimer formation. *Free. Radic. Biol. Med.* **104**, 262–271 (2017).
19. Liu, Y. Y., Nagpure, B. V., Wong, P. T. & Bian, J. S. Hydrogen sulfide protects SH-SY5Y neuronal cells against d-galactose induced cell injury by suppression of advanced glycation end products formation and oxidative stress. *Neurochem. Int.* **62**, 603–609 (2013).
20. Ghelani, H., Razmovski-Naumovski, V., Pragada, R. R. & Nammi, S. Attenuation of glucose-induced myoglobin glycation and the formation of advanced glycation end products (AGEs) by (R)- $\alpha$ -lipoic acid in vitro. *Biomolecules.* **8**, 9 (2018).
21. Mokhtari, S. *et al.* The attenuation of the toxic effects of LPS on mouse pre-implantation development by alpha-lipoic acid. *Theriogenology.* **143**, 139–147 (2020).
22. Qiu, X. *et al.* Alpha-lipoic acid regulates the autophagy of vascular smooth muscle cells in diabetes by elevating hydrogen sulfide levels. *Biochim. Biophys. Acta. Mol. Basis. Dis.* **1864**, 3723–3738 (2018).
23. Golestanfar, A. *et al.* Metabolic enhancement of the one carbon metabolism (OCM) in bovine oocytes IVM increases the blastocyst rate: evidences for a OCM checkpoint. *Sci. Rep.* **12**, 20629 (2022).
24. Dumoulin, J. C., Evers, J. L., Bras, M., Pieters, M. H. & Geraedts, J. P. Positive effect of taurine on preimplantation development of mouse embryos in vitro. *Reprod.* **94**, 373–380 (1992).
25. Pirotta, S. *et al.* Obesity and the risk of infertility, gestational diabetes, and type 2 diabetes in polycystic ovary syndrome. *Semin. Reprod. Med.* **38**, 342–351 (2020).
26. Ramlau-Hansen, C. H. *et al.* Subfecundity in overweight and obese couples. *Hum. Reprod.* **22**, 1634–1637 (2007).
27. Hutchison, J. C., Truong, T. T., Salamonsen, L. A., Gardner, D. K. & Evans, J. Advanced glycation end products present in the obese uterine environment compromise preimplantation embryo development. *Reprod. Biomed. Online.* **41**, 757–766 (2020).
28. Rabbani, N., Xue, M. & Thornalley, P. J. *Dicarbonyl stress and the glyoxalase system* (Oxidative Stress, 2020).
29. Lin, C. C. *et al.* Methylglyoxal activates NF- $\kappa$ B nuclear translocation and induces COX-2 expression via a p38-dependent pathway in synovial cells. *Life. Sci.* **149**, 25–33 (2016).
30. Cheng, A. S., Cheng, Y. H., Chiou, C. H. & Chang, T. L. Resveratrol upregulates Nrf2 expression to attenuate methylglyoxal-induced insulin resistance in Hep G2 cells. *J. Agric. Food. Chem.* **60**, 9180–9187 (2012).
31. Nishimoto, S., Koike, S., Inoue, N., Suzuki, T. & Ogasawara, Y. Activation of Nrf2 attenuates carbonyl stress induced by methylglyoxal in human neuroblastoma cells: Increase in GSH levels is a critical event for the detoxification mechanism. *Biochem. Biophys. Res. Commun.* **483**, 874–879 (2017).
32. Radmehr, V., Ahangarpour, A., Mard, S. A. & Khorsandi, L. Crocin attenuates endoplasmic reticulum stress in methylglyoxal-induced diabetic nephropathy in male mice: MicroRNAs alterations and glyoxalase 1-Nrf2 signaling pathways. *Iran. J. Basic Med. Sci.* **25**, 1341 (2022).
33. Kadlec, M., Ros-Santaella, J. L. & Pintus, E. The roles of NO and H<sub>2</sub>S in sperm biology: Recent advances and new perspectives. *Int. J. Mol. Sci.* **21**, 2174 (2020).
34. Wang, R. Physiological implications of hydrogen sulfide: a whiff exploration that blossomed. *Physiol. Rev.* **92**, 791–896 (2012).
35. Yang, C. T. *et al.* A novel controllable hydrogen sulfide-releasing molecule protects human skin keratinocytes against methylglyoxal-induced injury and dysfunction. *Cell. Physiol. Biochem.* **34**, 1304–1317 (2014).
36. Zhang, H. *et al.* Calcitriol prevents peripheral RSC96 Schwann neural cells from high glucose & methylglyoxal-induced injury through restoration of CBS/H<sub>2</sub>S expression. *Neurochem. Int.* **92**, 49–57 (2016).
37. Manna, P. & Jain, S. K. L-cysteine and hydrogen sulfide increase PIP3 and AMPK/PPAR $\gamma$  expression and decrease ROS and vascular inflammation markers in high glucose treated human U937 monocytes. *J. Cell. Biochem.* **114**, 2334–2345 (2013).
38. Al-Magableh, M. R., Kemp-Harper, B. K., Ng, H. H., Miller, A. A. & Hart, J. L. Hydrogen sulfide protects endothelial nitric oxide function under conditions of acute oxidative stress in vitro. *Naunyn-Schmiedeberg's Arch. Pharmacol.* **387**, 67–74 (2014).
39. Predmore, B. L., Lefer, D. J. & Gojon, G. Hydrogen sulfide in biochemistry and medicine. *Antioxid. Redox. Signal.* **17**, 119–140 (2012).
40. Whiteman, M. *et al.* Evidence for the formation of a novel nitrosothiol from the gaseous mediators nitric oxide and hydrogen sulfide. *Biochem. Biophys. Res. Commun.* **343**, 303–310 (2006).
41. Majumder, A. Targeting Homocysteine and Hydrogen Sulfide Balance as Future Therapeutics in Cancer Treatment. *Antioxid.* **12**, 1520 (2023).
42. Niu, G. *et al.*  $\alpha$ -lipoic acid can greatly alleviate the toxic effect of AGEs on SH-SY5Y cells. *Int. J. Mol. Med.* **41**, 2855–2864 (2018).

43. Huang, J. S., Chuang, L. Y., Guh, J. Y., Yang, Y. L. & Hsu, M. S. Effect of taurine on advanced glycation end products-induced hypertrophy in renal tubular epithelial cells. *Toxicol. Appl. Pharmacol.* **233**, 220–226 (2008).
44. Xu, M. *et al.* Taurine alleviates oxidative stress in porcine mammary epithelial cells by stimulating the Nrf2-MAPK signaling pathway. *Food. Sci. Nutr.* **11**, 1736–1746 (2023).
45. Esmaeli, F., Maleki, V., Kheirouri, S. & Alizadeh, M. The effects of taurine supplementation on metabolic profiles, pentosidine, soluble receptor of advanced glycation end products and methylglyoxal in adults with type 2 diabetes: A randomized, double-blind, placebo-controlled trial. *Can. J. Diabetes.* **45**, 39–46 (2021).
46. Nandhini, A. T., Thirunavukkarasu, V. & Anuradha, C. V. Stimulation of glucose utilization and inhibition of protein glycation and AGE products by taurine. *Acta. Physiol. Scand.* **181**, 297–303 (2004).
47. Mirani, M. *et al.* Pyridoxamine protects human granulosa cells against advanced glycation end-products-induced steroidogenesis disturbances. *Mol. Biol. Rep.* **50**, 1–3 (2023).
48. Taş, S., Sarandöl, E. & Dirican, M. Vitamin B6 supplementation improves oxidative stress and enhances serum paraoxonase/arylesterase activities in streptozotocin-induced diabetic rats. *Sci. World. J.* <https://doi.org/10.1155/2014/351598> (2014).
49. Voziyan, P. A. & Hudson, B. G. Pyridoxamine: the many virtues of a maillard reaction inhibitor. *Ann. N. Y. Acad. Sci.* **1043**, 807–816 (2005).
50. Booth, A. A., Khalifah, R. G. & Hudson, B. G. Thiamine pyrophosphate and pyridoxamine inhibit the formation of antigenic advanced glycation end-products: comparison with aminoguanidine. *Biochem. Biophys. Res. Commun.* **220**, 113–119 (1996).
51. Ramis, R. *et al.* How does pyridoxamine inhibit the formation of advanced glycation end products? The role of its primary antioxidant activity. *Antioxid.* **8**, 344 (2019).
52. Nakamura, S., Li, H., Adijiang, A., Pischetsrieder, M. & Niwa, T. Pyridoxal phosphate prevents progression of diabetic nephropathy. *Nephrol. Dial. Transplant.* **22**, 2165–2174 (2007).
53. Mascolo, E. & Verni, F. Vitamin B6 and diabetes: relationship and molecular mechanisms. *Int. J. Mol. Sci.* **21**, 3669 (2020).
54. Cao, Y. *et al.* Cystathionine  $\beta$ -synthase is required for oocyte quality by ensuring proper meiotic spindle assembly. *Cell. Prolif.* **55**, e13322 (2022).
55. Tural, R. *et al.* Investigation of oxidative stress status in cumulus cells in patients with in Vitro fertilization. *Turk. J. Med. Sci.* **51**, 1969–1975 (2021).
56. Tatemoto, H., Sakurai, N. & Muto, N. Protection of porcine oocytes against apoptotic cell death caused by oxidative stress during in vitro maturation: Role of cumulus cells. *Biol. Reprod.* **63**, 805–810 (2000).
57. Heydarnejad, A. *et al.* Supplementation of maturation medium with CoQ10 enhances developmental competence of ovine oocytes through improvement of mitochondrial function. *Mol. Reprod. Dev.* **86**, 812–824 (2019).

## Acknowledgements

The authors wish to express their great appreciation to the Department of Animal Science, Isfahan University of Technology, Isfahan, Iran, and Royan Institute for Biotechnology, Isfahan, Iran for their kind assistance in performing this study. In addition, we would like to acknowledge the contribution of the chat-based artificial intelligence tool in editing this article. While the content and writing of this article were primarily done by the authors themselves, chat-based AI was only used for editing purposes to enhance the clarity and coherence of the text.

## Author contributions

S. M: investigation, methodology, and writing-original draft; A.H.M: conceptualization, supervision and writing- review editing; F.J.: supervision, formal analysis, validation, and writing-original draft; M.R.: methodology; M.D. supervision and writing- review editing; M.H.N.E.: conceptualization, methodology, supervision, and writing- review editing.

## Competing interests

The authors declare no competing interests.

## Additional information

**Supplementary Information** The online version contains supplementary material available at <https://doi.org/10.1038/s41598-024-66785-5>.

**Correspondence** and requests for materials should be addressed to A.H.M. or M.H.N.-E.

**Reprints and permissions information** is available at [www.nature.com/reprints](http://www.nature.com/reprints).

**Publisher's note** Springer Nature remains neutral with regard to jurisdictional claims in published maps and institutional affiliations.



**Open Access** This article is licensed under a Creative Commons Attribution-NonCommercial-NoDerivatives 4.0 International License, which permits any non-commercial use, sharing, distribution and reproduction in any medium or format, as long as you give appropriate credit to the original author(s) and the source, provide a link to the Creative Commons licence, and indicate if you modified the licensed material. You do not have permission under this licence to share adapted material derived from this article or parts of it. The images or other third party material in this article are included in the article's Creative Commons licence, unless indicated otherwise in a credit line to the material. If material is not included in the article's Creative Commons licence and your intended use is not permitted by statutory regulation or exceeds the permitted use, you will need to obtain permission directly from the copyright holder. To view a copy of this licence, visit <http://creativecommons.org/licenses/by-nc-nd/4.0/>.

© The Author(s) 2024